Optimal resource allocation in cellular sensing systems

Christopher C. Govern and Pieter Rein ten Wolde[1]

FOM Institute AMOLF, Science Park 104, 1098 XG Amsterdam, The Netherlands

Edited by Yuhai Tu, IBM T. J. Watson Research Center, Yorktown Heights, NY, and accepted by the Editorial Board October 22, 2014 (received for review June 23, 2014)

Living cells deploy many resources to sense their environments, including receptors, downstream signaling molecules, time, and fuel. However, it is not known which resources fundamentally limit the precision of sensing, like weak links in a chain, and which can compensate each other, leading to trade-offs between them. We present a theory for the optimal design of the large class of sensing systems in which a receptor drives a push–pull network. The theory identifies three classes of resources that are required for sensing: receptors and their integration time, readout molecules, and energy (fuel turnover). Each resource class sets a fundamental sensing limit, which means that the sensing precision is bounded by the limiting resource class and cannot be enhanced by increasing another class—the different classes cannot compensate each other. This result yields a previously unidentified design principle, namely that of optimal resource allocation in cellular sensing. It states that, in an optimally designed sensing system, each class of resources is equally limiting so that no resource is wasted. We apply our theory to what is arguably the best-characterized sensing system in biology, the chemotaxis network of *Escherichia coli*. Our analysis reveals that this system obeys the principle of optimal resource allocation, indicating a selective pressure for the efficient design of cellular sensing systems.

cell signaling | thermodynamics | design principles | chemotaxis | information transmission

Biochemical networks are the information-processing devices of life. Like any device, they require resources to be built and run. Components are needed to construct the network, space is required to accommodate the components, time is needed to process the information, and energy is required to make the components and operate the network. These resources constrain the design and performance of any biochemical network. However, it is not clear which resources are indispensable, thus fundamentally limiting the performance of the network, and which resources might trade-off against each other. Here, we consider the interplay among cellular resources, network design, and performance in a canonical biochemical function, namely sensing the environment.

Living cells can measure chemical concentrations with extraordinary precision (1–3), raising the question what sets the fundamental limit to the accuracy of chemical sensing (1). Cells measure chemical concentrations via receptors on their surface. These measurements are inevitably corrupted by noise that arises from the stochastic arrival of ligand molecules by diffusion and from the stochastic binding of the ligand to the receptor. Berg and Purcell pointed out that the sensing error is fundamentally bounded by this noise extrinsic to the cell, but that cells can reduce the error by taking multiple independent measurements (1). One way to increase the number of measurements is to add more receptors (1, 4). Another is to take more measurements per receptor over time; here, the cell infers the concentration not from the instantaneous number of ligand-bound receptors, but rather from the average receptor occupancy over an integration time T (1, 4–11).

This time integration has to be performed by the signaling networks that transmit the information from the surface of the cell to its interior (10). Although the work of Berg and Purcell and subsequent studies identify time and the number of receptors as resources that limit the accuracy of sensing, the fundamental limits that have emerged ignore the cost of making and operating the signaling network. Making proteins is costly; producing proteins that confer no benefit to the cell can slow down bacterial growth (12). Moreover, many networks are driven out of thermodynamic equilibrium by the continuous turnover of fuel molecules such as ATP, leading to the dissipation of heat (13–17). In fact, one can estimate that the fuel needed to operate a sensory network is comparable to that to make new components after cell division (*SI Text*).

In this manuscript, we present a theory for the optimal design of sensing systems, which maximizes sensing precision given the available cellular resources. The theory applies to the large class of sensing systems in which a receptor drives a Goldbeter–Koshland push–pull network (18). These systems are ubiquitous in prokaryotic and eukaryotic cell signaling (19): examples include GTPase cycles, as in the Ras system, phosphorylation cycles, as in MAPK cascades, and two-component systems like the chemotaxis system of *Escherichia coli*.

We derive for this class of systems how the sensing accuracy depends on not only the number of receptors and their integration time, but also on the resources required to build and operate the downstream signaling network: the copies of signaling molecules and fuel. This allows us to address the following questions: How do the sensing limits set by the latter resources compare with the canonical limit of Berg and Purcell, which is set by the resources time and the number of receptors? How does the limit set by one resource depend on the levels of the other resources? Can resources compensate each other to achieve a desired sensing precision, leading to trade-offs between them, or are the limits set by the respective resources fundamental, i.e., independent of the levels of the other resources? In addition, what do these relationships imply for the optimal design of a system that maximizes sensing precision?

Significance

Cells continually have to sense their environments to make decisions—to stay put or move, to differentiate or proliferate, or even to live or die. However, they are thwarted by noise at the cellular scale. Cells use signaling networks to filter this noise as much as possible and sense accurately. To operate these networks, resources are required: time, protein copies, and energy. We present a theory for the optimal design of cellular sensing systems that maximize sensing precision given these resources. It reveals a new design principle, namely that of optimal resource allocation. It describes how these resources must be allocated so that none are wasted. We show that the chemotaxis network of *Escherichia coli* obeys this principle.

Author contributions: C.C.G. and P.R.t.W. designed research, performed research, and wrote the paper.

The authors declare no conflict of interest.

This article is a PNAS Direct Submission. Y.T. is a guest editor invited by the Editorial Board.

Freely available online through the PNAS open access option.

[1]To whom correspondence should be addressed. Email: tenwolde@amolf.nl.

This article contains supporting information online at www.pnas.org/lookup/suppl/doi:10.1073/pnas.1411524111/-/DCSupplemental.

We find that the resource limitations of these systems emerge naturally when the signaling networks are viewed as devices that discretely, rather than continuously, sample the receptor state via collisions of the signaling molecules with the receptor proteins. This analysis reveals that three classes of resources are required: (*i*) receptors and their integration time, (*ii*) copies of downstream molecules, and (*iii*) energy (fuel). Indeed, these classes cannot compensate each other: each imposes a sensing limit, and it is the limiting class that imposes the fundamental limit on the accuracy of sensing. However, there can be trade-offs within each class of resources. Receptors and integration time trade-off against each other in achieving a desired sensing accuracy, and power and response time trade-off against each other to meet the energy requirement for taking a measurement.

Our theory makes a strong prediction for the optimal design of sensing systems. Because the fundamental resource classes cannot compensate each other in achieving a desired sensing precision, any class that is not limiting the sensing precision is in excess and thus wasted. This naturally leads to a previously unidentified design principle, namely that of optimal resource allocation. It states that in an optimally designed sensing system each fundamental class of resources is equally limiting so that no resource is wasted. We test this prediction for the chemotaxis system of *Escherichia coli,* which is a specific example of the class of push–pull sensing systems (Fig. 1). Our analysis reveals that this network obeys the principle of optimal resource allocation. This indicates that there is a selective pressure on not only the topology of sensing networks that enhances robustness of adaptation (20–22), but also on the efficient allocation of cellular resources for precise sensing.

Results

Sensing at the Molecular Level. We consider a cell with R_T receptor proteins that independently bind ligand L, $R+L \rightleftharpoons RL$ (Fig. 2*A*). The receptor drives a push–pull network, which is a canonical nonequilibrium motif in prokaryotic and eukaryotic cell signaling

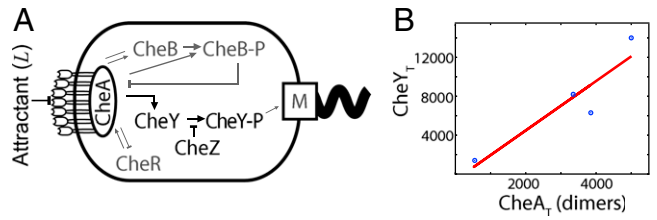

Fig. 1. The chemotaxis network of *E. coli* obeys the principle of optimal resource allocation, which states that in an optimally designed system each cellular resource is equally limiting. (*A*) Cartoon of the sensing system. The receptor is via the adaptor protein CheW associated with the kinase CheA. This complex, coarse-grained as *R* in our model, can bind extracellular ligand *L* and activate the intracellular messenger protein CheY (*x* in our model) by phosphorylating it; phosphorylated CheY controls the rotation direction of the motor. Deactivation, i.e., dephosphorylation, of CheY is catalyzed by the phosphatase CheZ; the effect of CheZ is coarse-grained into the deactivation rate. The proteins CheR and CheB, which implement adaptation, have been omitted, because we are interested in the lower bound on the accuracy of sensing in static environments. (*B*) The principle of optimal resource allocation, Eq. **5**, predicts that the number of CheY proteins, X_T, scales linearly with the number of receptor–CheA complexes, R_T, with a slope given by the relaxation time of the signaling network, τ_r, over the correlation time of the receptor ligand-binding state, τ_c. Plotted are data from ref. 23 for two *E. coli* strains under two different growth conditions; the number of CheA dimers is a proxy for the number of receptor–CheA complexes. The line is a best fit to the data, having a slope of ≈ 3. The resource allocation principle, Eq. **5**, thus predicts that $\tau_r/\tau_c \approx 3$. This is on the same order of magnitude as that given by the relaxation time, $\tau_r \approx 100$ ms (24), and correlation time $\tau_c \approx 10$ ms, estimated from the measured receptor–ligand dissociation constant (25) and association rate (26).

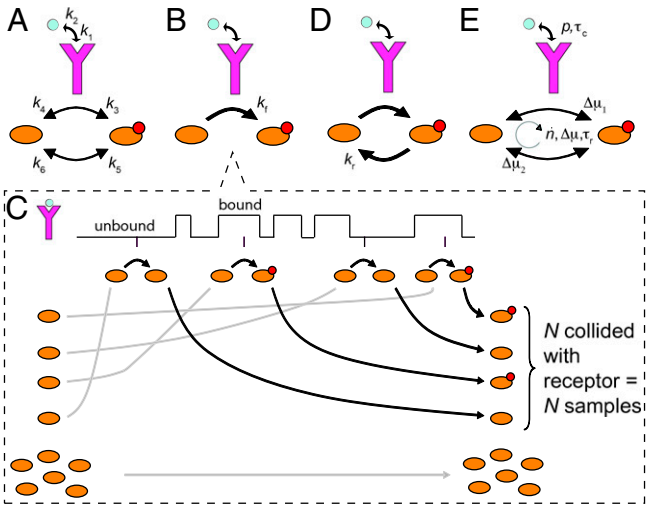

Fig. 2. Sensing at the molecular level. The sensing precision in terms of the rate constants $\{k_i\}$ (*A*) does not reveal the resource requirements (Eq. **S8**). To reveal these, the signaling network is viewed as a device that discretely samples the ligand-binding state of the receptor. The accuracy of sensing depends on how the samples are taken (*B* and *C*), erased (*D*), and on how reliable they are (*E*). (*B*) The ligand-bound receptor drives the modification of a downstream readout (i.e., the push–pull network $RL+x \rightarrow RL+x^*$). (*C*) The signaling network in *B* discretely samples the receptor state, illustrated for one receptor. The states of the receptor over time are encoded in the states of the *N* molecules that collided with it: the readout is modified if the receptor is bound; otherwise, it is unmodified. Molecules that collide with the unbound receptor are indistinguishable from those that have never collided, leading to an additional error. (*D*) Active molecules can be degraded, erasing samples. (*E*) All reactions are in principle reversible, compromising the encoding of the receptor state into the readout. The sensing error is determined by collective variables that reveal the resource requirements for sensing: the probability p that the receptor is bound to ligand, the receptor–ligand correlation time τ_c, the flux $\dot{n}$, the relaxation time τ_r, and the free-energy drops $\Delta\mu_1$ and $\Delta\mu_2$ across the activation and deactivation reactions of the readout, respectively.

(19). In these systems, the receptor itself or the enzyme associated with it, such as CheA in *E. coli* (Fig. 1), catalyzes the chemical modification of a readout protein x, such as CheY. Active readout molecules x^* can decay spontaneously or be deactivated by an enzyme, like the phosphatase CheZ in *E. coli.*

The cell infers the ligand concentration c from the instantaneous concentration of the output x^*, by inverting the mean input–output relation $\overline{x^*}(c)$. Linearizing $\overline{x^*}(c)$ and using error propagation, the expected fractional error in the concentration estimate is then as follows (1, 5, 11):

$$\left(\frac{\delta c}{c}\right)^2 = \frac{1}{c^2}\frac{\sigma^2_{x^*}}{\left(\frac{d\overline{x^*}}{dc}\right)^2}. \qquad [1]$$

The error is low if the readout responds sensitively to changes in ligand concentration, as measured by the gain $d\overline{x^*}/dc$, but is not noisy, as quantified by the variance $\sigma^2_{x^*}$.

We can compute $\sigma^2_{x^*}$ from the linear-noise approximation (*SI Text*), and using Eq. **1**, this yields Eq. **S8** for the sensing error. It is a complicated expression in terms of the eight fundamental variables in the system: the six rate constants describing the forward and reverse rates of the three reactions (including ligand–receptor binding), and the total copy numbers X_T and R_T (Fig. 2*A*).

Inspired by the analysis of a simpler system, we can arrive at a much more illuminating expression for the sensing error, by viewing the signaling network as a device that samples the receptor state

(*SI Text*). The general principle is that the activation reaction, $x+RL\xrightarrow{k_f}x^*+RL$ generates samples of the ligand-binding state of the receptor by storing the receptor state in the stable modification states of the readout molecules (Fig. 2 *B* and *C*). Readout molecules that collide with a ligand-bound receptor are activated, whereas those that collide with an unbound receptor remain inactive. In this way, each readout molecule that has interacted with the receptor provides a memory or sample of the ligand-occupation state of that receptor molecule; collectively, the readout molecules encode the history of the receptor states. Intuitively, we expect that if there are N receptor–readout interactions, then the cell has N samples of the receptor state and the error in the concentration estimate, $\delta c/c$, is reduced by a factor of $\sqrt{N}$, or less if the samples are not independent. To derive the effective number of independent samples, we need to consider not only the creation of samples, but also the erasure of samples and the quality of the samples (Fig. 2 *D* and *E*). The decay of the readout, $x^*\xrightarrow{k_r}x$ (Fig. 2*D*), is equivalent to discarding or erasing samples. Additionally, reactions are microscopically reversible, which means that readout activation can occur independently of the receptor, $x\xrightarrow{k_{-r}}x^*$, and receptor-mediated modifications can occur in the wrong direction, $x^*+RL\xrightarrow{k_{-f}}x+RL$ (Fig. 2*E*). These reverse reactions compromise the encoding of the receptor state into the readout: an active x^* molecule no longer encodes the ligand-bound state of the receptor at a previous time with 100% fidelity, because it could have been activated independently of the receptor; similarly, x, rather than x^*, may reflect a modification by a ligand-bound receptor. These reverse reactions thus reduce the reliability of a receptor sample. Energy is needed to break time reversibility and to protect the coding.

How receptor samples are taken (Fig. 2 *B* and *C*), erased (Fig. 2*D*), and how they are stored in the readout x (Fig. 2*E*), determine the number of receptor samples, their independence, and their accuracy, which together set the sensing precision (*SI Text*):

$$\left(\frac{\delta c}{c}\right)^2=\frac{1}{p(1-p)}\frac{1}{\overline{N}_I}+\frac{1}{(1-p)^2}\frac{1}{\overline{N}}. \qquad [2]$$

Here, p is the probability that a receptor is bound to ligand, and $1/(p(1-p))$ is the "instantaneous error," i.e., the sensing error based on a single concentration estimate via a single receptor. The quantity $\overline{N}_I$, discussed below, is the average number of samples that are independent. The second term, with $\overline{N}$ the total number of samples, accounts for the fact that the cell cannot distinguish between those molecules x that have collided with an unbound receptor (and hence provide information on the receptor occupancy), and those that have not collided with the receptor at all (Fig. 2*C*; *SI Text*). However, when p is small and/or $\overline{N}$ is large, the second term is small compared with the first. Eq. **2** then shows that the sensing error has a form that one would expect for a sampling protocol: the sensing error is that of an estimate based on a single concentration measurement, $1/(p(1-p))$, divided by the average number of independent measurements, $\overline{N}_I$.

The number of independent measurements $\overline{N}_I$ can be expressed in terms of collective variables that, as we will show, describe the resource limitations of the cell (Fig. 2*E*):

$$\overline{N}_I=\underbrace{\frac{1}{(1+2\tau_c/\Delta)}}_{f_I}\underbrace{\overbrace{\frac{(e^{\Delta\mu_1}-1)(e^{\Delta\mu_2}-1)}{e^{\Delta\mu}-1}}^{q}\overbrace{\frac{\dot{n}\tau_r}{p}}^{\overline{N}}}_{\overline{N}_{\mathrm{eff}}}. \qquad [3]$$

This expression has a clear interpretation. Cells count only those samples created less than a relaxation time τ_r in the past; nothing that happened earlier can influence the current state, including its ability to sense. Hence, τ_r is the effective integration time. The quantity $\dot{n}$ is the flux of x across the cycle of activation by the receptor and deactivation; it is given by $\dot{n}=k_f\bar{x}R_Tp-k_{-f}\overline{x^*}R_Tp$, where $\bar{x}$ and $\overline{x^*}$ are the average number of x and x^* in steady state. The product $\dot{n}\tau_r$ is thus the number of cycles of readout molecules involving collisions with ligand-bound receptor molecules during the system's relaxation time τ_r. The quantity $\dot{n}\tau_r/p$ is the total number of readout cycles involving collisions with receptor molecules, be they ligand bound or not. It is thus the total number of receptor samples taken during τ_r, $\overline{N}$.

Not all of these samples are reliable. The effective number of samples taken during τ_r is $\overline{N}_{\mathrm{eff}}=q\overline{N}$, where $0\le q\le 1$ measures the quality of each sample. Here, $\Delta\mu_1$ and $\Delta\mu_2$ are the average free-energy drops across the activation and deactivation pathway respectively, in units of k_BT (Fig. 2*E*); $\Delta\mu=\Delta\mu_1+\Delta\mu_2$ is the total free-energy drop across the cycle. When $\Delta\mu=\Delta\mu_1=\Delta\mu_2=0$, an active readout molecule is as likely to be created by the ligand-bound receptor as it is created spontaneously and there is no coding and no sensing; indeed, in this limit, $q=0$ and $\overline{N}_{\mathrm{eff}}=0$. In contrast, when $\Delta\mu_1,\Delta\mu_2\to\infty$, $q\to 1$ and $\overline{N}_{\mathrm{eff}}\to\overline{N}$.

The factor f_I denotes the fraction of samples that are independent. It depends on the correlation time τ_c of receptor–ligand binding and on the time interval $\Delta=2\tau_r/(\overline{N}_{\mathrm{eff}}/R_T)$ between samples of the same receptor. Samples farther apart are more independent.

Fundamental Resources and Trade-Offs. We can use Eqs. **2** and **3** to understand how cellular resources limit the precision of sensing. A resource or combination of resources that fundamentally limits sensing is a (collective) variable Q_i that, when fixed, puts a nonzero lower bound on the sensing error, no matter how the other variables are varied. A fundamental resource class Q_i is thus mathematically defined by the following: $\mathrm{MIN}_{Q_i=\mathrm{const}}(\delta c/c)^2=f(\mathrm{const})>0$. To find these classes, we numerically or analytically minimized the sensing error, constraining (combinations of) variables yet optimizing over the other variables. As we show in *SI Text*, when only $R_T\tau_r/\tau_c$ is constrained, $(\delta c/c)^2\ge 4/(R_T\tau_r/\tau_c)$; when only X_T is fixed, $(\delta c/c)^2\ge 4/X_T$; when only $\dot{w}\tau_r$ is limiting, $(\delta c/c)^2\ge 4/(\dot{w}\tau_r)$. When all resources are present in finite amounts, the minimum sensing error is set by the highest lower bound:

$$\left(\frac{\delta c}{c}\right)^2\ge\mathrm{MAX}\left(\frac{4}{R_T\tau_r/\tau_c},\frac{4}{X_T},\frac{4}{\dot{w}\tau_r}\right). \qquad [4]$$

Fig. 3 *A*–*C* shows that the resource classes $R_T\tau_r/\tau_c$, X_T, and $\dot{w}\tau_r$ are indeed fundamental: the minimum sensing error is bounded by the limiting class and cannot be reduced by increasing another resource. Clearly, increasing a single resource, e.g., X_T, cannot reduce the sensing error indefinitely. The sensing error will eventually plateau, namely when it becomes limited by another resource, e.g., $R_T\tau_r/\tau_c$. These fundamental resource classes thus cannot compensate for each other in achieving a required sensing precision and hence do not trade-off against each other. However, within these classes, trade-offs are possible. We now elucidate why the fundamental classes cannot compensate each other, whereas resources within a given class can, leading to trade-offs between them.

Time/Receptor Copy Numbers, $R_T\tau_r/\tau_c$. An independent sample of the same receptor can be taken roughly every $2\tau_c$. Naturally, samples can be taken more frequently. In fact, cells can time-integrate as in the theory of Berg and Purcell (1): if $X_T\to\infty$, the receptors are sampled infinitely fast and $\Delta\to 0$ and $\overline{N}_{\mathrm{eff}}\to\infty$. However, increasing X_T cannot reduce the sensing error ad infinitum, because the number of receptor samples that are independent will saturate at the Berg–Purcell factor, $R_T\tau_r/\tau_c$, and the sensing error $(\delta c/c)^2$ will plateau at $4/(R_T\tau_r/\tau_c)$. Indeed, $R_T\tau_r/\tau_c$ is the maximum number of independent concentration

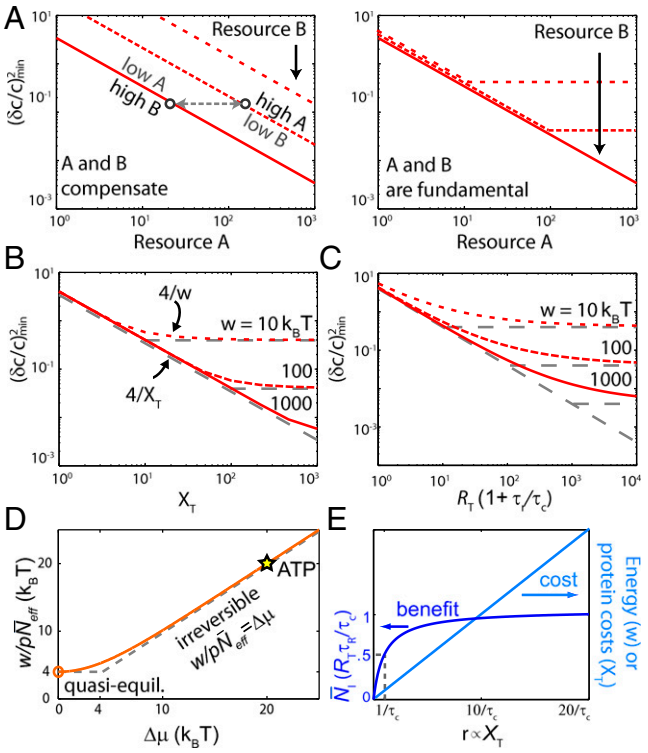

Fig. 3. Trade-offs in nonequilibrium sensing. (*A*) When two resources A and B compensate each other, one resource can always be decreased without affecting the sensing error, by increasing the other resource; concomitantly, increasing a resource will always reduce the sensing error. When both resources are instead fundamental, the sensing error is bounded by the limiting resource and cannot be reduced by increasing the other. (*B* and *C*) The three classes time/receptor copies, copies of downstream molecules, and energy are all required for sensing, with no trade-offs among them (Fig. 4). The minimum sensing error obtained by minimizing Eq. **2** is plotted for different combinations of (*B*) X_T and w, and (*C*) $R_T(1+\tau_r/\tau_c)$ and w (*SI Text*). The curves track the bound for the limiting resource indicated by the gray lines, showing that the resources do not compensate each other. The plot for the minimum sensing error as a function of $R_T(1+\tau_r/\tau_c)$ and X_T is identical to that of (*C*) with w replaced by X_T. (*D*) The energy requirements for sensing. In the irreversible regime ($\Delta\mu\to\infty$), the work to take one sample of a ligand-bound receptor, $w/(p\bar{N}_{\text{eff}})$, equals $\Delta\mu$, because each sample requires the turnover of one fuel molecule, consuming $\Delta\mu$ of energy. In the quasiequilibrium regime ($\Delta\mu\to 0$), each effective sample of the bound receptor requires $4k_BT$, which defines the fundamental lower bound on the energy requirement for taking a sample. When $\Delta\mu=0$, the network is in equilibrium and both w and $\bar{N}_{\text{eff}}$ are 0. ATP hydrolysis provides $20k_BT$, showing that phosphorylation of readout molecules makes it possible to store the receptor state reliably. The results are obtained from Eq. **3** with $\Delta\mu_1=\Delta\mu_2=\Delta\mu/2$. (*E*) Sampling more than once per correlation time requires more resources, although the benefit is marginal. As the sampling rate is increased by increasing the readout copy number X_T, the number of independent measurements $\bar{N}_I$ saturates at the Berg–Purcell limit $R_T\tau_r/\tau_c$, but the energy consumption and protein cost ($\propto X_T$) continue to rise.

measurements—the total number of receptors R_T times the maximum number of independent measurements per receptor τ_r/τ_c. This shows that there is no fundamental relationship between sensing and receptor copy number: the latter can be traded against time to reach a desired sensing precision. Essentially, the error is determined by the total number of samples and it does not matter, as long as the samples are independent, whether these samples are from the same receptor over time or from many receptors at the same time.

Downstream Readout Molecules, X_T. The concentration measurements need to be stored in the readout molecules. Each readout molecule provides at most one sample, because at any given time it exists in only one modification state, regardless of how many times it has collided with the receptor or how long the integration time τ_r is. There is no mechanistic sense in which a single molecule "integrates" the receptor state. As a consequence, no matter how the network is designed, how much time or energy it uses, or how many receptors it has, cells are fundamentally limited by the pool of readout molecules: the sensing error $(\delta c/c)^2 \geq 4/X_T$.

Energy, $\dot{w}\tau_r$. The free-energy drop across a cycle, $\Delta\mu$, must be provided by a fuel molecule such as ATP. The power, the rate at which the fuel molecules do work, is $\dot{w}=\dot{n}\Delta\mu$, and the total work performed during τ_r is $w\equiv\dot{w}\tau_r$. This work is spent on taking samples of receptor molecules that are bound to ligand, because only they can modify downstream readout molecules. Hence, the work needed to take one effective sample of a ligand-bound receptor is $w/(p\bar{N}_{\text{eff}})$, with $\bar{N}_{\text{eff}}$ given by Eq. **3**. Fig. 3*D* shows this quantity as a function of $\Delta\mu$. While $w/(p\bar{N}_{\text{eff}})=\Delta\mu/q$ increases continuously with $\Delta\mu$, two limiting regimes can be observed.

When $\Delta\mu > 4k_BT$, the work to take one effective sample of a ligand-bound receptor becomes simply $w/(p\bar{N}_{\text{eff}})=\Delta\mu$. In this regime, the readout reactions are essentially irreversible, $q\to 1$, and each sample requires the turnover of one fuel molecule, using $\Delta\mu$ of energy. Energy limits the accuracy of sensing, not because it limits the reliability q of each sample, but because it limits the total number of samples $\bar{N}_{\text{eff}}=\dot{n}\tau_r/p$ by limiting the receptor sampling frequency $\dot{n}$: $(\delta c/c)^2\geq 1/(\dot{n}\tau_r)=\Delta\mu/(\dot{w}\tau_r)$. Intriguingly, this bound suggests that for a fixed amount of energy, $w=\dot{w}\tau_r$, spent during the relaxation time τ_r, the sensing error can be reduced to zero by reducing $\Delta\mu$ to zero. However, this lower bound only applies when $q\to 1$, i.e., when $\Delta\mu > 4k_BT$.

When $\Delta\mu < 4k_BT$, the system transitions to a quasiequilibrium regime in which each fuel molecule provides a small but nonzero amount of energy. In this regime, the system can still consume significant amounts of energy when the fuel molecules are consumed at a rapid rate $\dot{n}$ by many distinct readout molecules. In the limit that $\dot{n}\to\infty$ and $\Delta\mu\to 0$ at fixed $\dot{w}=\dot{n}\Delta\mu$, the effective number of samples given by Eq. **3** reduces to $\bar{N}_{\text{eff}}\to\dot{w}\tau_r/(4p)$. Each readout–receptor interaction corresponds to an increasingly noisy measurement of the receptor state ($q\to 0$), but many noisy measurements ($\bar{N}=\dot{n}\tau_r/p\to\infty$) contain the same information as 1 perfect measurement—provided that collectively at least $4k_BT$ was spent on them. Indeed, as Fig. 3*D* shows, $4k_BT$ is the fundamental lower bound on the work needed to take one accurate sample of a ligand-bound receptor. It puts another bound on the sensing error: $(\delta c/c)^2\geq 4/(\dot{w}\tau_r)$. The bound can be reached when $R_T\tau_r/\tau_c$ and X_T are not limiting, and $\Delta\mu\to 0$.

Eq. **4** shows that the sensing precision depends on the work done in the past relaxation time, $w=\dot{w}\tau_r$, setting up a trade-off among speed, power, and accuracy, as found in adaptation (13). When the response needs to be rapid, τ_r needs to be small and the power demand is high: the samples, which require energy, must be taken close together in time. However, when the cell can wait a long time τ_r before responding, the power $\dot{w}$ required to make w large can be infinitesimal: the samples can be created far apart in time. There is no minimum power requirement for sensing.

Optimal Resource Allocation. Because the fundamental resource classes cannot compensate each other in achieving a desired sensing precision, any class that is in excess of the minimum amount necessary to achieve that precision is wasted. For example, the benefit of sampling the receptor faster by increasing X_T in reducing the sensing error saturates, whereas the total protein and energetic costs continue to rise with X_T (Fig. 3*E*). To the extent that all resources affect growth, evolutionary pressure should tend to drive systems so that no resource is wasted, which

occurs when all are equally limiting. Resource-optimal systems sample the receptor about once per correlation time and use just enough fuel and downstream molecules to do so. Quantitatively, from Eq. **4**, all resources are equally limiting when

$$R_T\tau_r/\tau_c \approx X_T \approx w. \qquad [5]$$

In an optimal sensing system, the number of independent concentration measurements $R_T\tau_r/\tau_c$ equals the number of readout molecules X_T that store these measurements and equals the work (in units of k_BT) to create the samples.

Comparison with Experiment. Eq. **5** makes a strong prediction for the optimal design of the large class of sensing systems that are based on the push–pull motif. We can test this prediction for the chemotaxis system of *E. coli* (Fig. 1), which has been well characterized experimentally. In this system, the receptor forms a complex with the kinase CheA. This complex, which is coarse-grained into R, can bind the ligand L and activate the intracellular messenger protein CheY (x) by phosphorylating it. Deactivation of CheY is catalyzed by CheZ, the effect of which is coarse-grained into the deactivation rate (*SI Text*).

The number of chemotaxis proteins depends on the growth rate: the number of receptors and CheY proteins varies as much as 10-fold as a function of strain and growth medium (23). Interestingly, however, these variations occur in concert for all components and thus hardly change their relative amounts (23). This is the scaling behavior predicted by Eq. **5**, assuming that τ_r is robust to variations in the growth rate.

Not only the scaling of the number of CheY proteins, X_T, with the number of receptor–CheA complexes, R_T, can be tested, but also the magnitude of their ratio. A fit of the data of Li and Hazelbauer, shown in Fig. 1*B*, shows that $X_T/R_T \approx 3$ for different strains and growth media (23). Eq. **5** thus predicts that $\tau_r/\tau_c \approx 3$. The relaxation rate τ_r^{-1} is ≈ 2 s^{-1} for the attractant response and ≈ 20 s^{-1} for the repellent response (24), yielding $\tau_r \approx 100$ ms. Hence, Eq. **5** predicts that $\tau_c \approx 30$ ms. This prediction can be tested, assuming that the correlation time τ_c of the receptor–CheA complex is that of receptor–ligand binding. Specifically, we can estimate τ_c from the receptor–ligand dissociation rate k_{off} as $\tau_c \simeq 1/(2k_{\text{off}})$, $(p \approx 0.5)$. The dissociation constant of Tar-aspartate (receptor–ligand) binding $K_D \approx 0.1$ μM (25), and with an association rate $k_{\text{on}} \approx 10^9 \text{M}^{-1}\cdot\text{s}^{-1}$ (26), this yields $k_{\text{off}} \approx 100$ s^{-1} and an estimated correlation time $\tau_c \approx 10$ ms, in line with the prediction of Eq. **5**.

Eq. **5** also predicts that the total number of CheY molecules X_T equals the chemical work $w = \dot{n}\Delta\mu\tau_r$ (in units of k_BT) to phosphorylate CheY during τ_r. In steady state, the flux $\dot{n}$ of CheY phosphorylation balances the flux of CheYp dephosphorylation. The latter equals the inverse lifetime $\tau_l^{-1} \approx \tau_r^{-1}$ times the number of CheYp molecules in steady state, αX_T, where α is the fraction of CheY that is phosphorylated. This yields $w \approx \alpha\Delta\mu X_T$. The fraction $\alpha \approx 0.16$ (24). CheY phosphorylation is driven by ATP hydrolysis, which means that $\Delta\mu = 20k_BT$. Hence $w \approx 3X_T$, thus on the order of X_T, as Eq. **5** predicts. We thus argue that in the chemotaxis system of *E. coli*, the resources are optimally allocated, i.e., according to Eq. **5**.

Discussion

Fig. 4 summarizes our analysis. The sensing precision is limited by three classes of resources. The resource class time/receptors $R_T\tau_r/\tau_c$ determines the maximum total number of independent concentration measurements that can be taken. However, these measurements need to be stored in downstream molecules. Moreover, energy is needed to store the samples reliably and to protect the coding. These three classes of resources are indeed fundamental. The sensing error is bounded by the limiting class like the weakest link in a chain, and other classes cannot compensate

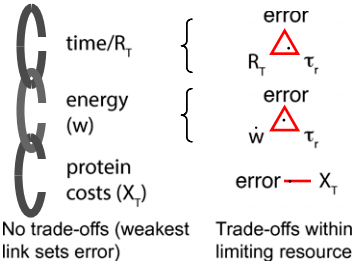

Fig. 4. The relationship between resources and the precision of biochemical sensing. The sensing precision is fundamentally limited by time and receptor copies, energy, and copies of downstream readouts. These three classes of resources cannot compensate each other, and it is the limiting resource that sets the fundamental limit to the precision of sensing. Within each class, however, trade-offs are possible: Power can be traded against speed to meet the energy requirement for reaching a desired sensing accuracy, whereas time can be traded against the number of receptors.

for it. For example, adding receptors and readout molecules does not improve sensing if not enough energy is used to take the samples (Fig. 3*B*); similarly, waiting more time to take another sample is not beneficial if the cell has no more readout molecules left to write the sample to, or cannot expend energy fast enough to accomplish the writing (Fig. 3*C*). However, within the fundamental resource classes, trade-offs are possible: time can be traded against the number of receptors to reach a required number of measurements, whereas power can be traded against speed to meet the energy requirement for a desired sensing accuracy. These design principles are in marked contrast to those of equilibrium sensing systems, which are not driven out of equilibrium via fuel turnover: the sensing precision of these systems is limited by the number of receptors; downstream networks can never improve the accuracy of sensing (27).

We find that at least $4k_BT$ is needed for reliably encoding a measurement. One of the most widely used coding strategies is phosphorylation, which requires ATP. In vivo, ATP hydrolysis provides about $20k_BT$. This is sufficient to take one receptor sample essentially irreversibly (Fig. 3*D*), which means that q reaches unity. Readout phosphorylation thus makes it possible to store the receptor state reliably.

Nonequilibrium networks can exhibit more complicated features than those of the simple push–pull motif, as in the MAPK cascade. The molecular picture for time integration suggests that our results hold generally, even in these more complicated systems. Indeed, we find the same or more severe resource limitations in signaling cascades and in networks with simple negative or positive feedback (*SI Text*). Although cascades can increase the response time (10), which increases information transfer, they do not make sensing more efficient in terms of energy or readout molecules.

In an optimally designed system, each fundamental resource is equally limiting. This leads to a specific prediction for the design of an optimal sensing system: the integration time, energy, and copy numbers of receptor and readout should satisfy Eq. **5**. Importantly, this design principle of optimal resource allocation is independent of the resource costs. This is because the sensing precision is bounded by the limiting resource class; resources that are in excess cannot improve sensing and are thus wasted, no matter how cheap they are. Fig. 3 *C* and *D* show that, even close to the optimum where all resources are equally limiting, the minimum error closely follows the lower bound of Eq. **4** (*SI Text*), supporting the idea that Eq. **5** is indeed fairly insensitive to the resource costs. It explains perhaps why Eq. **5** so successfully predicts the design of the *E. coli* chemotaxis system.

The optimal trade-off between nonfundamental resources within the fundamental resource classes will depend on their

fitness costs and benefits. For example, how receptors are traded against time in reaching a desired sensing precision will depend on the benefit of a fast response time and the cost of making the receptor proteins.

To understand how *E. coli* moves in a concentration gradient, we have to understand not only how the sensing system filters high-frequency ligand-binding noise by time averaging the receptor state—the topic of this study—but also how, on much longer timescales, the adaptation system computes the change in the concentration and filters low-frequency noise induced by the cell's random motion in the concentration gradient (28). Recently, Lan et al. (13) found a trade-off between the speed, power, and accuracy of adaptation, which mirrors the trade-off between power, speed, and precision of sensing observed here. Interestingly, the adaptation and sensing system share the receptor. In fact, the adaptation system continually performs work to keep the receptor activity close to 0.5. There is thus an energetic adaptation cost associated with the receptors, in addition to the energetic cost of synthesizing them. This adaptation cost will affect the trade-off between the nonfundamental resources receptors and time. It will not, however, affect the design principle of optimal resource allocation, which is based on the fundamental resource classes and hence insensitive to resource costs.

Whether other sensing systems satisfy the design principle of Eq. **5** remains an interesting question. Two-component systems are ideal for testing this once kinetic data and protein expression levels become available (29). Eq. **5** not only makes predictions for individual systems but also predicts that the fundamental resources should vary proportionally to each other across different systems. For example, the relation predicts that the lifetime τ_r of the modified readout should increase, *ceteris parabus*, with its expression level X_T. The design principle of Eq. **5** can also be used to construct optimal synthetic networks that minimize resource consumption.

Finally, the process of sampling a time series, like the receptor state over time, defines a specific, familiar computation that could be conducted by any machine; it is instantiated in the biochemical system by the readout–receptor pair. We find that the free-energy drops across the "measurement" and "erasure" steps, $\Delta\mu_1$ and $\Delta\mu_2$, should be identical to minimize the energetic cost, even though the fuel molecule need only be involved in one of the reactions, preparing a nonequilibrium state that relaxes via the other. This allocation of energy differs from that typically considered in the computational literature, in which only the erasure step requires energy (30). In the cellular system, both steps are computational erasures: although only the erasure step erases memory of the receptor state, both steps erase the state of the molecule involved in the collision. Interestingly, when $p = 0.5$, the average work to measure the state of the receptor is $2k_BT$, which is perhaps surprisingly close to the Landauer bound, $k_BT\ln(2)$ (30).

ACKNOWLEDGMENTS. We thank Andew Mugler, Thomas Ouldridge, and Tom Shimizu for critical readings of sections of the manuscript. This work is part of the research programme of the Foundation for Fundamental Research on Matter (FOM), which is part of the Netherlands Organisation for Scientific Research (NWO).

1. Berg HC, Purcell EM (1977) Physics of chemoreception. *Biophys J* 20(2):193–219.
2. Sourjik V, Berg HC (2002) Receptor sensitivity in bacterial chemotaxis. *Proc Natl Acad Sci USA* 99(1):123–127.
3. Ueda M, Shibata T (2007) Stochastic signal processing and transduction in chemotactic response of eukaryotic cells. *Biophys J* 93(1):11–20.
4. Wang K, Rappel WJ, Kerr R, Levine H (2007) Quantifying noise levels of intercellular signals. *Phys Rev E Stat Nonlin Soft Matter Phys* 75(6 Pt 1):061905.
5. Bialek W, Setayeshgar S (2005) Physical limits to biochemical signaling. *Proc Natl Acad Sci USA* 102(29):10040–10045.
6. Rappel WJ, Levine H (2008) Receptor noise and directional sensing in eukaryotic chemotaxis. *Phys Rev Lett* 100(22):228101.
7. Endres RG, Wingreen NS (2009) Maximum likelihood and the single receptor. *Phys Rev Lett* 103(15):158101.
8. Hu B, Chen W, Rappel WJ, Levine H (2010) Physical limits on cellular sensing of spatial gradients. *Phys Rev Lett* 105(4):048104.
9. Mora T, Wingreen NS (2010) Limits of sensing temporal concentration changes by single cells. *Phys Rev Lett* 104(24):248101.
10. Govern CC, ten Wolde PR (2012) Fundamental limits on sensing chemical concentrations with linear biochemical networks. *Phys Rev Lett* 109(21):218103.
11. Kaizu K, et al. (2014) The Berg-Purcell limit revisited. *Biophys J* 106(4):976–985.
12. Dekel E, Alon U (2005) Optimality and evolutionary tuning of the expression level of a protein. *Nature* 436(7050):588–592.
13. Lan G, Sartori P, Neumann S, Sourjik V, Tu Y (2012) The energy-speed-accuracy tradeoff in sensory adaptation. *Nat Phys* 8(5):422–428.
14. De Palo G, Endres RG (2013) Unraveling adaptation in eukaryotic pathways: Lessons from protocells. *PLoS Comput Biol* 9(10):e1003300.
15. Mehta P, Schwab DJ (2012) Energetic costs of cellular computation. *Proc Natl Acad Sci USA* 109(44):17978–17982.
16. Barato AC, Hartich D, Seifert U (2013) Information-theoretic versus thermodynamic entropy production in autonomous sensory networks. *Phys Rev E Stat Nonlin Soft Matter Phys* 87(4):042104.
17. Skoge M, Naqvi S, Meir Y, Wingreen NS (2013) Chemical sensing by nonequilibrium cooperative receptors. *Phys Rev Lett* 110(24):248102.
18. Goldbeter A, Koshland DE, Jr (1981) An amplified sensitivity arising from covalent modification in biological systems. *Proc Natl Acad Sci USA* 78(11):6840–6844.
19. Alon U (2007) *Introduction to Systems Biology: Design Principles of Biological Networks* (CRC Press, Boca Raton, FL).
20. Barkai N, Leibler S (1997) Robustness in simple biochemical networks. *Nature* 387(6636):913–917.
21. Alon U, Surette MG, Barkai N, Leibler S (1999) Robustness in bacterial chemotaxis. *Nature* 397(6715):168–171.
22. Kollmann M, Løvdok L, Bartholomé K, Timmer J, Sourjik V (2005) Design principles of a bacterial signalling network. *Nature* 438(7067):504–507.
23. Li M, Hazelbauer GL (2004) Cellular stoichiometry of the components of the chemotaxis signaling complex. *J Bacteriol* 186(12):3687–3694.
24. Sourjik V, Berg HC (2002) Binding of the *Escherichia coli* response regulator CheY to its target measured in vivo by fluorescence resonance energy transfer. *Proc Natl Acad Sci USA* 99(20):12669–12674.
25. Vaknin A, Berg HC (2007) Physical responses of bacterial chemoreceptors. *J Mol Biol* 366(5):1416–1423.
26. Danielson MA, Biemann HP, Koshland DE, Jr, Falke JJ (1994) Attractant- and disulfide-induced conformational changes in the ligand binding domain of the chemotaxis aspartate receptor: A ^{19}F NMR study. *Biochemistry* 33(20):6100–6109.
27. Govern CC, ten Wolde PR (2014) Energy dissipation and noise correlations in biochemical sensing. *Phys Rev Lett*, in press.
28. Sartori P, Tu Y (2011) Noise filtering strategies in adaptive biochemical signaling networks: Application to *E. coli* chemotaxis. *J Stat Phys* 142(6):1206–1217.
29. Gao R, Stock AM (2013) Probing kinase and phosphatase activities of two-component systems in vivo with concentration-dependent phosphorylation profiling. *Proc Natl Acad Sci USA* 110(2):672–677.
30. Landauer R (1961) Irreversibility and heat generation in the computing process. *IBM J Res Develop* 5(3):183–191.

Supporting Information

Govern and ten Wolde 10.1073/pnas.1411524111

SI Text

The Fuel Needed to Drive the *Escherichia coli* Chemotaxis Network Is Comparable to That to Make New Components After Cell Division

Below, we address the question: How does the ATP cost of driving the *E. coli* chemotaxis sensing system compare with the energetic cost of making the components of this system?

Estimating Energetic Cost of Protein Production. The number of ATP molecules required to make a protein is approximately five per amino acid [BioNumbers ID 106158 (1)]. Table S1 reports the copy number ranges for key chemotaxis proteins and their molecular weight. These proteins need to be synthesized during the cell cycle to balance the loss upon cell division. Assembling these numbers, about 2–8 $\times$ 10^7 ATP are required to produce chemotaxis proteins over the cell cycle.

Estimating Energetic Cost of Driving the Chemotaxis Network. The chemotaxis network of *E. coli* is modeled as follows (2):

$$A \xrightarrow{k_A} Ap, \qquad \text{[S1]}$$

$$Ap + Y \xrightarrow{k_f} A + Yp, \qquad \text{[S2]}$$

$$Yp \xrightarrow{k_r} Y, \qquad \text{[S3]}$$

where A and Ap denote the unphosphorylated and phosphorylated forms of CheA, and Y and Yp the unphosphorylated and phosphorylated forms of CheY.

The reactions imply that in steady state:

$$k_A\left([A_T]-[Ap]\right)=k_f[Ap]\left([Y_T]-[Yp]\right)=k_r[Yp]=\dot{n}. \qquad \text{[S4]}$$

The second and third terms in this equation (and thus the first) are expressions for the flux of CheY, $\dot{n}$, in steady state. The lifetime of CheYp is $\tau_l \approx 100$ ms (2), which is the inverse of k_r in our model: $k_r \approx 10/s$. A similar estimate for k_r can be obtained by noting that the deactivation is mediated by CheZ and calculating k_r from Michaelis–Menten kinetics as $k_r=(k_{cat}[Z][Yp])/(K_m+[Z])$ using parameters in ref. 2. The total turnover rate $\dot{n}$ is thus $10/s$ times the number of CheYp molecules. About a sixth of the 1,000–8,000 CheY molecules are phosphorylated in the steady state (2). Then the number of CheYp is roughly 200–1,500. The total turnover rate $\dot{n}$ is thus 2,000–15,000 molecules per second, which is also the ATP turnover rate, because the phosphorylation reaction is essentially irreversible. If the cell cycle time is about an hour (3,600 s), the turnover of ATP is about 1–5 $\times$ 10^7 ATP per cell cycle.

From these calculations, we see that the ATP cost of driving the chemotaxis sensing machinery ($\approx$1–5 $\times$ 10^7 ATP per cell cycle) is comparable to the energetic cost of making the components of the sensing machinery ($\approx$2–8 $\times$ 10^7). This comparison depends critically on the growth rate of the cell and protein expression levels, which can vary in different media. Furthermore, it does not account for the energy to drive or build other components of the chemotaxis pathway, such as the flagella or the adaptation machinery. However, it provides an order-of-magnitude comparison, which suggests that the energy to drive a signaling pathway can be comparable to the cost of making the components of that pathway.

Calculating the Sensing Error for a Biochemical Network

From Eq. **1** in the main text, the sensing error for a biochemical network depends on the gain and the variance of the readout. We have calculated the gains using a mean-field approximation for the steady-state level of the readout. We have calculated all variances using a linear-noise approximation (3). For nonlinear networks, the quality of the approximation improves with system size; it can already be quite good for systems with only 10 copies of each molecule (4).

The linear-noise approximation gives the covariance matrix Σ for stationary fluctuations in species' levels as the solution to the Lyapunov equation:

$$A\Sigma+\Sigma A^T+B=0, \qquad \text{[S5]}$$

where $A=S^T\nabla\nu$ and $B=S^T\mathrm{Diag}(\nu)S$ in terms of the stoichiometric matrix S and the reaction propensity vector ν. The stoichiometric matrix describes how many molecules of each species are consumed or produced in each reaction, and the propensity vector describes the propensity (rate) of each reaction. For a network out of steady state (as in *Base Model: Taking Samples via Readout Activation* below), a nonstationary version must be used (3).

Langevin Approximation to the Dynamics of a Biochemical Network

The Langevin approximation to the dynamics of a biochemical network draws on the same framework as the linear-noise approximation (3). It expresses the fluctuations in species copy numbers $\boldsymbol{N}$ as follows:

$$\frac{d\boldsymbol{N}}{dt}=A\boldsymbol{N}+\eta(t), \qquad \text{[S6]}$$

where $\boldsymbol{N}$ is a vector containing the copy numbers of all species and $\eta(t)$ are Gaussian noises, uncorrelated in time, with covariance B. A and B are the matrices defined in *Calculating the Sensing Error for a Biochemical Network*. The equation can be solved [e.g., by integrating factors (3)], yielding the result in the main text, Eq. **3**, for the biochemical network considered there.

Derivation of Eqs. 2 and 3 of the Main Text

The principle is that the cell infers the concentration c from the instantaneous output x^*, by inverting the input–output relation $\overline{x^*}(c)$. Linearizing the input–output relation, and using error propagation, the fractional error of the concentration estimate is given by the following (5–7):

$$\left(\frac{\delta c}{c}\right)^2=\frac{1}{c^2}\frac{\sigma_{x^*}^2}{\left(\frac{d\overline{x^*}}{dc}\right)^2}. \qquad \text{[S7]}$$

We can compute the variance of the output x^*, $\sigma_{x^*}^2$, using the linear-noise approximation to the master equation (see above, *Calculating the Sensing Error for a Biochemical Network*). Using the above expression, this yields the following:

$$\left(\frac{\delta c}{c}\right)^2 = \Bigg(\Bigg((k_1+k_2)^4 \left(k_{-\mathrm{r}} + k_{\mathrm{r}} + \frac{k_1\left(k_{\mathrm{f}}+k_{-\mathrm{f}}\right)R_T}{k_1+k_2} \right) \times \left(\left(k_{-\mathrm{r}} + \frac{k_1 k_{\mathrm{f}} R_T}{k_1+k_2} \right) \left(k_{\mathrm{r}} + \frac{k_1 k_{-\mathrm{f}} R_T}{k_1+k_2} \right) \left(k_{-\mathrm{r}} + k_{\mathrm{r}} + \frac{k_1\left(k_{\mathrm{f}}+k_{-\mathrm{f}}\right)R_T}{k_1+k_2} \right) + \frac{k_1 k_2 \left(k_{-\mathrm{f}}k_{-\mathrm{r}} - k_{\mathrm{f}}k_{\mathrm{r}}\right)^2 R_T X_T}{(k_1+k_2)\left((k_1+k_2)(k_1+k_2+k_{-\mathrm{r}}+k_{\mathrm{r}}) + k_1\left(k_{\mathrm{f}}+k_{-\mathrm{f}}\right)R_T\right)} \right) \Bigg) \Big/ \left(k_1^2 k_2^2 \left(k_{-\mathrm{f}}k_{-\mathrm{r}} - k_{\mathrm{f}}k_{\mathrm{r}}\right)^2 R_T^2 X_T \right) \Bigg). \quad \textbf{[S8]}$$

Here, $k_1 = \tilde{k_1} L$ (with L the ligand concentration) and k_2 are the rate constants for ligand binding and unbinding from the receptor, respectively, k_{f} is the rate of receptor-mediated phosphorylation, $k_{-\mathrm{f}}$ is the microscopically reverse reaction, k_{r} is the rate of dephosphorylation, $k_{-\mathrm{r}}$ is the microscopically reverse reaction, and R_T and X_T are the number of receptor and readout molecules, respectively. Clearly, the above expression is not very illuminating.

Eqs. **2** and **3** of the main text are much more illuminating. They describe the sensing error not in terms of the rate constants, but in terms of the collective variables $p, \tau_c, \tau_r, \dot{n}, \Delta\mu_1, \Delta\mu_2, \Delta$ that describe the resource limitations of the cell. The inspiration for the form of these expressions came from an analysis of a simpler network. We describe this analysis in the subsection below. Here, we first repeat Eqs. **2** and **3** for completeness, and then describe how it can be verified that they indeed correspond to Eq. **S8**.

Eqs. **2** and **3** of the main text are as follows:

$$\left(\frac{\delta c}{c}\right)^2 = \frac{1}{p(1-p)}\frac{1}{\overline{N}_I} + \frac{1}{(1-p)^2}\frac{1}{\overline{N}} \quad \textbf{[S9]}$$

and

$$\overline{N}_I = \underbrace{\frac{1}{(1+2\tau_c/\Delta)}}_{f_I} \underbrace{\frac{\overbrace{\left(e^{\Delta\mu_1}-1\right)\left(e^{\Delta\mu_2}-1\right)}^{q}}{e^{\Delta\mu}-1} \overbrace{\frac{\dot{n}\tau_r}{p}}^{\overline{N}}}_{\overline{N}_{\mathrm{eff}}}. \quad \textbf{[S10]}$$

To see the correspondence between Eqs. **S9** and **S10** (i.e., Eqs. **2** and **3** of the main text) and Eq. **S8**, note that variables in Eqs. **S9** and **S10** can be expressed in terms of the rate constants as follows:

$$p = \frac{\tilde{k_1}L}{\tilde{k_1}L + k_2} = \frac{k_1}{k_1+k_2}, \quad \textbf{[S11]}$$

$$\tau_c = \frac{1}{\tilde{k_1}L + k_2} = \frac{1}{k_1+k_2}, \quad \textbf{[S12]}$$

$$\tau_r = \frac{1}{k_{-\mathrm{r}} + k_{\mathrm{r}} + k_{\mathrm{f}} p R_T + k_{-\mathrm{f}} p R_T}, \quad \textbf{[S13]}$$

$$\dot{n} = k_{\mathrm{f}}\overline{RL}\,\bar{x} - k_{-\mathrm{f}}\overline{RL}\,\overline{x^*} = \frac{\left(k_{\mathrm{f}}k_{\mathrm{r}} - k_{-\mathrm{f}}k_{-\mathrm{r}}\right)pR_T X_T}{k_{-\mathrm{r}} + k_{\mathrm{r}} + \left(k_{\mathrm{f}}+k_{-\mathrm{f}}\right)pR_T}, \quad \textbf{[S14]}$$

$$\Delta\mu_1 = \log\frac{k_{\mathrm{f}}\bar{x}}{k_{-\mathrm{f}}\overline{x^*}} = \log\frac{k_{\mathrm{f}}\left(k_{\mathrm{r}} + k_{-\mathrm{f}}pR_T\right)}{k_{-\mathrm{f}}\left(k_{-\mathrm{r}} + k_{\mathrm{f}}pR_T\right)}, \quad \textbf{[S15]}$$

$$\Delta\mu_2 = \log\frac{k_{\mathrm{r}}\overline{x^*}}{k_{-\mathrm{r}}\bar{x}} = \log\frac{k_{\mathrm{r}}\left(k_{-\mathrm{r}} + k_{\mathrm{f}}pR_T\right)}{k_{-\mathrm{r}}\left(k_{\mathrm{r}} + k_{-\mathrm{f}}pR_T\right)}, \quad \textbf{[S16]}$$

$$\Delta = 2\tau_r/\left(\overline{N}_{\mathrm{eff}}/R_T\right) = \frac{2\left(k_{-\mathrm{f}}k_{-\mathrm{r}} - k_{\mathrm{f}}k_{\mathrm{r}}\right)\bar{x}\overline{x^*}}{\left(k_{\mathrm{f}}\bar{x} - k_{-\mathrm{f}}\overline{x^*}\right)^2\left(k_{-\mathrm{r}}\bar{x} - k_{\mathrm{r}}\overline{x^*}\right)} = \frac{2\left(k_{-\mathrm{r}} + k_{\mathrm{f}}pR_T\right)\left(k_{\mathrm{r}} + k_{-\mathrm{f}}pR_T\right)\left(k_{-\mathrm{r}} + k_{\mathrm{r}} + \left(k_{\mathrm{f}}+k_{-\mathrm{f}}\right)pR_T\right)}{\left(k_{-\mathrm{f}}k_{-\mathrm{r}} - k_{\mathrm{f}}k_{\mathrm{r}}\right)^2 pR_T X_T}. \quad \textbf{[S17]}$$

The relaxation time τ_r is calculated from the eigenvalues of the A matrix defined in *Calculating the Sensing Error for a Biochemical Network*. The free-energy drops are calculated following ref. 8. Substituting the expressions for these variables into Eqs. **S9** and **S10** (i.e., Eqs. **2** and **3** of the main text) yields Eq. **S8** in terms of the rate constants.

The Inspiration for Eqs. 2 and 3 of the Main Text: The Signaling Network Viewed as a Sampling Device. The inspiration for Eq. **2** of the main text (Eq. **S9**) came from an analysis of a simpler system. For this simpler system, we can analytically obtain the sensing error by viewing the signaling network as a device that samples the receptor state. As we will show below, the expression for the sensing error in this simpler model (Eq. **S18**) has exactly the same form as Eq. **2** of the main text (Eq. **S9**), corresponding to the full system. Indeed, Eq. **S18** provided the motivation to cast the expression for the sensing error of the full system (Eq. **S8**) in the form of Eq. **2** of the main text (Eq. **S9**).

We introduce this simpler model step by step: we first describe how samples are taken, and then how samples are erased. The derivation of the sensing error using the perspective of sampling is relegated to the appendices; below, we give the results. We then extend the model to discuss the effect of the finite pool of readout molecules and the reliability of the samples. In doing so, we will arrive at the full model of the main text.

Base Model: Taking Samples via Readout Activation. We consider a cell that responds at time T to a change in ligand concentration at an earlier time $t=0$, based on the output x^* of the simple reaction network $x + RL \xrightarrow{k_{\mathrm{f}}} x^* + RL$ (Fig. 2*B* of the main text). We assume that the cell starts with a large pool of inactive readout molecules x and that activated molecules x^* are never deactivated. For descriptive ease, we assume the reaction is diffusion-limited, so that each collision between an inactive molecule x and a ligand-bound receptor leads to activation of x.

Readout molecules that collide with the receptor over time are modified depending on the ligand-occupation state of the receptor. The total rate at which inactive molecules collide with receptor molecules in any state (be they ligand bound or not) is $r = k_{\mathrm{f}} x R_T \approx k_{\mathrm{f}} X_T R_T$ for a large readout pool, and the total number of such collisions after time T is N, with $\overline{N} = rT$ on average. If a receptor molecule is bound to ligand at the time of a collision, the readout molecule is converted to its active form, whereas if it is not the readout remains unchanged. In this way, the state of the receptor at the time of a collision is encoded in the state of the readout molecule that collided with it, and the history of the receptor states is encoded in the states of the readout molecules at the time T (Fig. 2*C*). The readout molecules that collided with the receptor thus constitute samples of the receptor state. The average number of samples after time T is $\overline{N} = rT = k_{\mathrm{f}} X_T R_T T$—the product of the total number of receptors R_T and the number of samples per receptor $k_{\mathrm{f}} X_T T$ during the integration time T.

The resulting sensing error can be derived via Eq. **1** of the main text (i.e., Eq. **S7**) from the chemical master equation, which describes fluctuations in the network (see *Calculating the Sensing Error for a Biochemical Network*, noting that the linear-noise approximation is exact for linear networks). The same expression can also be derived independently by viewing the signaling network as a system that samples the receptor state and using tools from discrete stochastic processes. This supports the idea that the signaling network truly samples the ligand-binding state of the receptor. This analysis is given in *Appendix A*. Here, we give the result. Interestingly, the sensing error for the base model has exactly the same form as Eq. **2** of the main text (Eq. **S9**) for the full model:

$$\left(\frac{\delta c}{c}\right)^2 = \frac{1}{p(1-p)}\frac{1}{\overline{N}_I} + \frac{1}{(1-p)^2}\frac{1}{\overline{N}}. \qquad \textbf{[S18]}$$

Here, as in the main text, $\overline{N}$ is the total number of samples and $\overline{N}_I$ is the number of samples that are independent. The latter is given by the following:

$$\overline{N}_I = f_I\overline{N} = \frac{1}{1+\dfrac{2\tau_c}{\Delta}}\overline{N}, \qquad \textbf{[S19]}$$

when $T \gg \tau_c$. Here, $f_I = 1/(1+(2\tau_c/\Delta))$ is the fraction of samples that is independent, which depends on the receptor–ligand correlation time τ_c and the time interval $\Delta \equiv T/(\overline{N}/R_T) = 1/(k_f X_T)$ between samples of the same receptor. This expression shows that the finite sampling rate r reduces the number of independent samples below the Berg–Purcell factor $R_T T/(2\tau_c)$, the maximum number of independent samples that can be taken during T. The latter is reached only when the sampling rate is infinite (e.g., the number of downstream molecules $X_T \to \infty$), so that $\overline{N} \to \infty$ and $\Delta \to 0$.

Erasing Samples via Readout Deactivation. The error in Eq. **S18** decreases with the time T, suggesting that the cell can sense perfectly if it waits long enough before responding to a change in its environment. However, modification states of molecules decay, and their finite lifetime, τ_l, limits sensing, regardless of how long the cell waits. To explore this at the molecular level, we consider the network in the previous paragraph augmented with the deactivation reaction, $x^* \xrightarrow{k_r} x$, $k_r = 1/\tau_\ell$ (Fig. 2*D* of the main text). We consider the sensing error after long times ($T \gg \tau_\ell$), in steady state, again for a large pool of inactive readout molecules. For pedagogical clarity, we imagine the deactivation is mediated by a phosphatase and that the reaction is diffusion-limited.

We can calculate the sensing error by solving the master equation or by viewing the system as one that discretely samples the receptor state, as described in *Appendix A*. It shows that the sensing error is again given by Eq. **S18**. However, the number of samples is lower than that in the case without deactivation, $\overline{N} = r\tau_\ell < rT$, and they are spaced effectively farther apart, $\Delta = 2\tau_\ell/(\overline{N}/R_T) = 2/(k_f X_T) > 1/(k_f X_T)$. The molecular picture of sampling provides a clear interpretation. As before, the readout molecules encode the state of a receptor and serve as samples of the receptor state. With deactivation, however, only those readout molecules that have collided with the receptor more recently than with the phosphatase reflect the receptor state. At any given time, the average number of such readout molecules, and hence samples, is $\overline{N} = r\tau_\ell$; the lifetime τ_ℓ thus sets an effective integration time. As without deactivation, the fraction f_I of samples that are independent is determined by the effective spacing Δ between them. Although the time between the creation of samples is still $1/(k_f X_T)$, i.e., the spacing without readout deactivation, some of the samples are erased via collision with the phosphatase. We therefore expect that the spacing between remaining samples is larger. Indeed, calculating the effective spacing between samples taking this effect into account yields $\Delta = 2/(k_f X_T)$, which is twice that without decay (*Appendix B*).

Beyond the Simple Model: Finite Pool of Readout Molecules. The copy numbers of signaling molecules are often small. To take this into account, we compute the sensing error from Eq. **1** of the main text for a finite number of readout molecules X_T using the linear-noise approximation to the master equation describing the biochemical fluctuations (see *Calculating the Sensing Error for a Biochemical Network*). Again, the sensing error can be written in the form given by Eqs. **S18** and **S19**. This defines an effective number of samples, $\overline{N} = r\tau_r$, where r is, as before, the receptor sampling rate, and τ_r is the relaxation time of the network. The sampling rate $r = k_f \bar{x} R_T$, whereas $\tau_r = 1/(k_f p R_T + k_r)$. In essence, cells count only those samples created less than a relaxation time in the past; nothing that happened earlier can influence the current state, including its ability to sense. The fraction of samples that is independent is given by Eq. **S19** with $\Delta = 2\tau_r/(\overline{N}/R_T) = 2/(k_f \bar{x})$, analogously to the previous paragraph.

Reliability of the Samples: The Full Model. All reactions are in principle microscopically reversible. Taking this into account, we recognize that active molecules that collide with the bound receptor sometimes become inactive, $x^* + RL \xrightarrow{k_{-f}} x + RL$, and that inactive molecules that collide with the phosphatase are sometimes activated, $x \xrightarrow{k_{-r}} x^*$ (Fig. 2*E* of the main text). These reverse reactions compromise the encoding of the receptor state into the readout, as described in the main text: an active x^* molecule no longer encodes the ligand-bound state of the receptor at a previous time with 100% reliability, because it can also result from a collision with the phosphatase; similarly, x, rather than x^*, may reflect a collision with the ligand-bound receptor.

Taking the reverse reactions into account, the full model of the main text is given by the following reactions:

$$R + L \underset{k_2}{\overset{k_1}{\rightleftharpoons}} RL, \qquad \textbf{[S20]}$$

$$RL + x \underset{k_{-f}}{\overset{k_f}{\rightleftharpoons}} RL + x^*, \qquad \textbf{[S21]}$$

$$x^* \underset{k_{-r}}{\overset{k_r}{\rightleftharpoons}} x. \qquad \textbf{[S22]}$$

From Eqs. **2** and **3** of the main text (Eqs. **S9** and **S10**), it is seen that the error in the full model with reversible reactions has the same form as Eq. **S18** above, but with the effective number of independent samples $\overline{N}_I$ given by Eq. **S10**: $\overline{N}_I = f_I q \overline{N}$, where q is the quality factor of the sample. The quality factor q is zero when the network is not driven out of equilibrium and reaches unity when the network is driven far out of equilibrium. In the latter case, when $q \to 1$, this model reduces to that of the previous paragraph. Indeed, in this irreversible limit, the effective number of samples $\overline{N}_{\text{eff}}$ as defined by Eq. **3** of the main text is $\overline{N}_{\text{eff}} = \overline{N} = \dot{n}\,\tau_r/p = r\tau_r = k_f \bar{x} R_T \tau_r$, with the flux $\dot{n}$ in Eq. **3** of the main text reducing to rp, with p, the probability that a receptor is bound to ligand, and $r = k_f \bar{x} R_T$, the rate at which the receptor is sampled in the irreversible model of the previous paragraph.

Derivation of Eq. 4 of the Main Text

Resources or combinations of resources that fundamentally limit sensing, are those (collective) variables Q_i that, when fixed, set a lower nonzero bound on the sensing error, no matter how the other variables in the system are varied. If we denote all of the eight variables in the system by

$k=\{k_1,k_2,k_f,k_{-f},k_r,k_{-r},R_T,X_T\}$, then the fundamental variables Q_i are defined by the following:

$$\mathrm{MIN}_{k:Q_i=\mathrm{const}}(\delta c/c)^2=f(\mathrm{const})>0. \quad \textbf{[S23]}$$

To find these fundamental collective variables, we numerically or analytically minimized the sensing error, constraining combinations of variables yet allowing the other variables not to be limiting. This procedure identified three fundamental resource classes: $Q_1=R_T\tau_R/\tau_c$, $Q_2=X_T$, and $Q_3=\dot{w}\tau_r$. Each class puts a fundamental lower bound on the sensing error, which means that the sensing error is limited by the value of Q_i and cannot be reduced to zero by increasing another variable. We now derive the sensing limits for the respective resource classes.

Receptors and Their Integration Time, $R_T\tau_r/\tau_c$, Limiting. When only $R_T\tau_r/\tau_c$ is constrained, the other resources can be optimized. The sensing error is minimized when the system is strongly driven out of equilibrium, $\Delta\mu_1,\Delta\mu_2\gg 0$. The receptor samples are then stored in the readout x with 100% fidelity and the quality factor reaches unity, $q\to 1$ (see Eq. **3** of the main text or Eq. **S10** above). In this limit, we can ignore the microscopically reverse reactions, and the readout flux $\dot{n}=k_f\bar{x}R_Tp-k_{-f}\bar{x}^*R_Tp$ reduces to $\dot{n}=k_f\bar{x}R_Tp$. This is indeed the rate at which the readout x is activated by ligand-bound receptor; it is thus the rate at which samples of the ligand-bound receptor are taken. The total number of samples of the receptor $\overline{N}=\dot{n}\tau_r/p$ obtained during the integration time τ_r therefore reduces to $\overline{N}=k_f\bar{x}R_T\tau_r$. Because $q=1$, this is also the effective number of samples: $\overline{N}_{\mathrm{eff}}=\overline{N}=k_f\bar{x}R_T\tau_r$. The sensing error is minimized when X_T and $\bar{x}$ become infinite. The number of samples $\overline{N}_{\mathrm{eff}}$ then becomes infinite, but the spacing between the samples $\Delta=2\tau_r/(\overline{N}_{\mathrm{eff}}/R_T)=2/(k_f\bar{x})$ becomes zero. Consequently, the number of independent samples becomes $\overline{N}_I=R_T\tau_r/\tau_c$ (see Eq. **3** or Eq. **S10**). Indeed, in the limit that the receptors and their integration time are limiting, the number of independent measurements $\overline{N}_I$ reaches the Berg–Purcell factor, i.e., the number of receptors R_T times the number of independent measurements per receptor τ_r/τ_c. The bound on the sensing error is given by the first term of Eq. **2** of the main text or Eq. **S9** above, which with $\overline{N}_I=R_T\tau_r/\tau_c$ yields the following:

$$\left(\frac{\delta c}{c}\right)^2_{R_T\tau_r/\tau_c}\geq\frac{1}{p(1-p)R_T\tau_r/\tau_c}\geq\frac{4}{R_T\tau_r/\tau_c}, \quad \textbf{[S24]}$$

because the maximum of $p(1-p)$ is 0.25, obtained when $p=0.5$.

Number of Readout Molecules X_T Limiting. The bound associated with the second resource class X_T can be derived from Eqs. **2** and **3** of the main text (Eqs. **S9** and **S10** above), but perhaps the most straightforward derivation is directly from Eq. **1** of the main text (i.e., Eq. **S7** above). When X_T becomes limiting, the variance of x is dominated by the intrinsic binomial switching noise—the extrinsic contribution from the receptor becomes vanishingly small. This gives $\sigma^2_{x^*}=f(1-f)X_T$, where $f=pk_fR_T/(pk_fR_T+k_r)$ is the fraction of X_T that is phosphorylated. The gain $\partial\bar{x}^*/\partial c=X_Tf(1-f)(1-p)/c$. Together, this yields from Eq. **1** of the main text (Eq. **S7** above):

$$\left(\frac{\delta c}{c}\right)^2_{X_T}=\frac{1}{f(1-f)(1-p)^2X_T}\geq\frac{4}{X_T}. \quad \textbf{[S25]}$$

Energy w Is Limiting. In the scenario that $w=\dot{w}\tau_r=\dot{n}\Delta\mu\tau_r$ is limiting and the other resources are in abundance, $f_I=1$ and $\overline{N}_I=\overline{N}_{\mathrm{eff}}=q\dot{n}\tau_r/p=qw/(p\Delta\mu)$ (see Eq. **3** of the main text and Eq. **S10** above). The number of samples of ligand-bound receptor per amount of work w is $p\overline{N}_{\mathrm{eff}}/w=q/\Delta\mu$. It is maximized when $\Delta\mu_1=\Delta\mu_2=\Delta\mu/2$ and $\Delta\mu\to 0$. In this limit, the work to take one effective sample of a ligand-bound receptor reaches its lower bound of $4k_BT$: $w/(p\overline{N}_{\mathrm{eff}})=4$, as described in the main text. The number of independent measurements in this limit is $\overline{N}_I=w/(4p)$. Together with Eq. **2** of the main text (Eq. **S9** above), this yields the following:

$$\left(\frac{\delta c}{c}\right)^2_w\geq\frac{4}{(1-p)w}\geq\frac{4}{w}. \quad \textbf{[S26]}$$

When all resources are present in finite amounts, the minimum sensing error is given by the highest of the above lower bounds. This yields Eq. **4** of the main text:

$$\left(\frac{\delta c}{c}\right)^2\geq\mathrm{MAX}\left(\frac{4}{R_T\tau_r/\tau_c},\frac{4}{X_T},\frac{4}{\dot{w}\tau_r}\right). \quad \textbf{[S27]}$$

The resource classes $R_T\tau_r/\tau_c$, X_T, and $\dot{w}\tau_r$ are indeed fundamental. They each set a fundamental lower bound on the sensing error, which cannot be beaten by increasing another resource. For example, when $R_T\tau_r/\tau_c$ is constrained, the minimum sensing error can never be lower than the bound given by Eq. **S24**, no matter how much X_T is increased or no matter how much the power $\dot{w}$ is raised. In contrast, R_T is not fundamental: for a given R_T, the sensing error can be reduced to zero by increasing τ_r. Similarly, the work w is fundamental: for a given w, the sensing error can never be lower than the bound set by Eq. **S26**. The power $\dot{w}$, however, is not fundamental: for a given $\dot{w}$, the error can be reduced to zero by increasing the integration time. Finally, we note that the factors 4 in Eqs. **S24–S26** have a common origin: for each resource class, the optimal consumption of the resource occurs when it is equally partitioned into two pools: optimal allocation of energy occurs when the total energy drop is equally partitioned into the energy drops of activation and deactivation; the receptors are optimally allocated when one-half of them is ligand bound; and the readout pool is optimally allocated when it is equally partitioned between active and inactive molecules.

Connection with Optimal Resource Allocation Principle of Eq. 5 of the Main Text

Eq. **4** of the main text (Eq. **S27**) indentifies the fundamental resource classes in cellular sensing systems. These resource classes cannot compensate each other in achieving a desired sensing precision, which is illustrated in Fig. 3 of the main text (how this figure is generated is described in the section below). Fig. 3 shows that the minimum sensing error tracks the highest of the lower bounds of Eqs. **S24–S26**: the minimum sensing error is set by the limiting resource class. This observation leads to the design principle of optimal resource allocation embedded in Eq. **5** of the main text, which states that, in an optimally designed system, all fundamental resource classes are equally limiting so that none is wasted. Importantly, this design principle does not depend on the relative costs of the resources. The reason is that fundamental resources that are in excess, cannot improve sensing and are thus wasted, no matter how cheap they are. Close to the optimum where all resources are equally limiting, the precise costs of the resources may become important, because, as Fig. 3 shows, close to the optimum there is, e.g., via the receptor, cross talk between the fundamental resource classes in setting the sensing precision: at the intersection of the dashed gray lines corresponding to the lower bounds of the respective resource classes, the minimum error (red line) is higher than the lower bound given by Eq. **S27**—as expected, the minimum sensing error crosses over smoothly from one bound to another, and not discontinuously. However, as Fig. 3 shows, even in the crossover regime the minimum error (red line) is never much higher than the lower bound of Eq. **S27** (the dashed-gray lines). Even close to the optimum, the mutual dependence between the resource classes is

thus small. It is probably for this reason that the optimal resource allocation principle of Eq. **5**, which does not rely on resource costs, gives such a surprisingly accurate prediction of the quantitative relationship between the number of receptors, readout molecules, integration time, receptor correlation time, and energy in the *E. coli* chemotaxis system.

Fig. 3 of the Main Text: No Trade-Offs Among Resource Classes

In Fig. 3*B* of the main text, we show how the sensing error depends on the pair of resources (readout copy number X_T, energy w). These results were obtained via numerical minimization of Eqs. **2** and **3** of the main text subject to constraints on X_T and w.

In Fig. 3*C* of the main text, we show how the sensing error depends the pair of resources (time/receptor copy number, energy). The plot for (time/receptor copy number, readout copy number) is the same. In this section, we describe the derivation of the results shown in this figure. To consider τ_r/τ_c not necessarily large, we need to use a form of the Berg–Purcell bound that is valid for short integration times (9):

$$\left(\frac{\delta c}{c}\right)^2_{\min} > \frac{1}{p(1-p)}\,\frac{1}{R_T\left(1+\dfrac{\tau_r}{\tau_c}\right)}, \qquad \text{[S28]}$$

which identifies $R_T(1+\tau_r/\tau_c)$ as a limiting resource, rather than the result of the main text, $R_T\tau_r/\tau_c$, which only holds in the limit $\tau_r \gg \tau_c$.

To elucidate how the sensing error depends on (time/receptor copy number, energy) and (time/receptor copy number, readout copy number), we calculate the minimum sensing error by optimizing over all parameters while fixing $R_T(1+\tau_r/\tau_c)$ and either w or X_T, respectively. For a fixed $R_T(1+\tau_r/\tau_c)$ and a fixed work w, the minimum sensing error is as follows:

$$\begin{aligned}\left(\frac{\delta c}{c}\right)^2_{\min} = \frac{w}{32}\Bigg(&-\frac{1}{\left(R_T\left(1+\frac{\tau_r}{\tau_c}\right)\right)^2}\\ &+\sqrt{\frac{1}{R_T\left(1+\frac{\tau_r}{\tau_c}\right)}\left(\frac{1}{R_T\left(1+\frac{\tau_r}{\tau_c}\right)}+\frac{32}{w}\right)}^{3/2}\\ &+\frac{128}{w^2}+\frac{80}{w\left(R_T\left(1+\frac{\tau_r}{\tau_c}\right)\right)}\Bigg).\end{aligned} \qquad \text{[S29]}$$

The equation for the dependence of the sensing error on (time/receptor copy number, readout copy number) is the same, with w replaced by X_T. The minimum is plotted in Fig. 3*C*. The minimum tracks the worst bound, again showing that the resources do not compensate each other.

Additional constraints on the values of rate constants will generally prevent the network from achieving these bounds. In particular, it is common to consider that the binding of ligand to receptor is diffusion-limited, so that the bound $4/(R_T(1+\tau_r/\tau_c))$ is never achieved. Of course, additional constraints cannot improve the performance of the network beyond the bounds required here, nor can they alter the fact that all of the resources are needed for sensing.

Additional Networks

Networks are often more complicated than a simple one-level push–pull cascade. We investigate some common motifs to understand whether they relax the trade-offs faced by sensory networks.

Multilevel Cascades. Often the signaling molecule activated by the receptor is not taken as the final readout; rather that molecule catalyzes the activation of another molecule, and so on in a signaling cascade. All of the molecules are reversibly degraded. Using the same approach as for the one-level cascade, we find that the sensing error is bounded by the work done driving just the last step of the cascade: $\overline{N}_{\text{eff}} \le \dot{w}_i\tau_r/(4p)$, where $\dot{w}_i = \dot{n}_i\Delta\mu_i$ is the product of the flux of the last molecule through its cycle and the free-energy drop across that cycle, and τ_r is the slowest relaxation time in the cascade (i.e., the reciprocal of the largest eigenvalue of the relaxation matrix). Even more work is done at other levels of the cascade. The results suggest that cascades do not enable more energy efficient sensing. Additionally, each sample of an active state (bound receptor or active molecule upstream) still requires a molecule to store it.

Positive and Negative Feedback. A simple model of positive feedback is autocatalysis, in which the receptor-catalyzed activation of the readout is enhanced by the activated form of the readout, x^*: $x + x^* + RL \rightleftharpoons 2x^* + RL$. A simple model of negative feedback can be implemented by requiring inactive x for the activation: $2x + RL \rightleftharpoons x + x^* + RL$. In both cases, x^* degrades according to $x^* \rightleftharpoons x$. Neither positive feedback nor negative feedback changes the energetic requirements for sensing: $\overline{N}_{\text{eff}} = (\dot{n}\tau_r/p)(e^{\Delta\mu_1}-1)(e^{\Delta\mu_2}-1)/(e^{\Delta\mu-1})$. As before, the free-energy drops across the reactions were calculated as the ratio of mass–action propensities.

Cooperative Activation of the Readout. If the catalytic activation of the readout is mediated cooperatively by the receptors (i.e., $x + nRL \rightleftharpoons x^* + nRL$), then the error is reduced by a factor n^2 for the same amount of energy. One way to interpret the result is that each sample requires the same amount of energy as before, but the samples are individually more informative because they reflect n ligand bindings, instead of one—indeed, the instantaneous error is lower.

Appendix A: Discretely Sampling the Receptor State

In this appendix, we show for the simple model consisting of $x + RL \xrightarrow{k_f} x^* + RL$ and $x^* \xrightarrow{k_r} x$, how the sensing error can be calculated by viewing the network as a discrete sampling device. The important quantities in a sampling protocol are the number of samples taken and the spacing between them, in addition to the properties of the sampled signal. By viewing the biochemical process as a sampling process, we mean that the underlying parameters of the biochemical network affect the sensing error only insofar as they affect these quantities, or the stochasticity in these quantities. The benefit of viewing the network as a sampling process is that the number of samples and the spacing between them have intuitive, and well-known, effects on the sensing error: the more samples, the lower the error; the further apart the samples are, the more independent they are. Perhaps less well known are the effects on the sensing error of stochasticity in the number of samples or the spacing between samples; these effects emerge in the process of determining the error for a discrete sampling protocol, which we do below.

We consider the base model of readout activation, $x + RL \xrightarrow{k_f} x^* + RL$, and the base model of readout activation plus readout deactivation, $x + RL \xrightarrow{k_f} x^* + RL$ and $x^* \xrightarrow{k_r} x$. For the base model, we indentify the molecules that have collided with the receptors as samples, because these molecules' states reflect the receptor states at the times of their collisions with the receptor. For the model with deactivation, we identify the molecules that

collided with the receptor more recently than with the phosphatase as samples. When we refer to the number of samples, we mean the number of these molecules; when we refer to the times of the samples, we mean the times at which these molecules collided with the receptor.

We begin by rewriting the equation for the sensing error in a form that makes the connection to discrete sampling explicit, Eq. **S33** below. The cell senses its environment through the level of its readout x^*. However, this is no different from estimating the ligand concentration from $\hat{p} = x^*/\overline{N}$:

$$\left(\frac{\delta c}{c}\right)^2 = \frac{\sigma_{\hat{p}}^2}{\left(\frac{d\bar{p}}{d\mu_L}\right)^2} = \frac{\sigma_{\bar{x}^*}^2}{\left(\frac{d\bar{x}^*}{d\mu_L}\right)^2}, \qquad \textbf{[S30]}$$

because $\overline{N}$ is a constant, independent of μ_L. Note that the gain $d\bar{p}/d\mu_L$ is $d\bar{p}/d\mu_L = p(1-p)$.

We first consider the effect of the stochasticity in the total number of samples, N. The law of total variance allows us to decompose the variance in the estimate $\hat{p}$ into terms arising from different sources:

$$\sigma_{\hat{p}}^2 = E\left[\mathrm{var}(\hat{p}|N)\right] + \mathrm{var}\left[E(\hat{p}|N)\right]. \qquad \textbf{[S31]}$$

The first term of Eq. **S31** reflects the mean of the variance in $\hat{p}$ given the number of samples N; the second term reflects the variance of the mean of $\hat{p}$ given the number of samples N.

The mean and variance of $\hat{p}$ given the number of samples N are more familiar quantities than their unconditioned counterparts, as we see below. Because, by definition, the samples reflect the state of the receptor at the times t_i of their collisions with the receptor, we can write the number of x^* at the final time as follows:

$$x^* = \sum_{i=1}^{N} n_i(t_i), \qquad \textbf{[S32]}$$

where $n_i(t_i)$ denotes the value of the ith sample—the state of the receptor involved in the ith collision at the time t_i of that collision, 1, if bound to ligand, and 0, otherwise. In the following, we consider a single receptor, $R_T = 1$ and $n = n_i$. The results generalize to multiple receptors.

We can then rewrite Eq. **S31** as follows:

$$\sigma_{\hat{p}}^2 = E\left[\frac{N^2}{\overline{N}^2}\mathrm{var}\left(\frac{\sum_{i=1}^{N} n(t_i)}{N}\middle| N\right)\right] + \mathrm{var}\left[\frac{N}{\overline{N}}E\left(\frac{\sum_{i=1}^{N} n(t_i)}{N}\middle| N\right)\right]. \qquad \textbf{[S33]}$$

The equation is a bit complicated, but what is important is that it fully specifies the sensing error in terms of the number of samples, the spacings between them, and the stochasticity in these quantities. That is, this equation shows that the sensing error is the error of a sampling process. We can use it to calculate the sensing error independently from, for example, the master equation or the linear-noise approximation.

The first term describes the error of a very standard sampling process, one with a fixed number of samples. We recognize the variance,

$$\mathrm{var}\left(\frac{\sum_{i=1}^{N} n(t_i)}{N}\middle| N\right), \qquad \textbf{[S34]}$$

as the error of a statistical sampling protocol in which exactly N samples are taken at random times t_i. This is shown explicitly in *Appendix B*. In that appendix, it is shown that the error for such a sampling protocol is as follows:

$$\mathrm{var}\left(\frac{\sum_{i=1}^{N} n(t_i)}{N}\middle| N\right) = p(1-p)\frac{1}{f_I N}, \qquad \textbf{[S35]}$$

where f_I is the fraction of the samples that are independent, as given by Eq. **S19**. Then the first term in Eq. **S33** is just the following:

$$E\left[\frac{N^2}{\overline{N}^2}\mathrm{var}\left(\frac{\sum_{i=1}^{N} n(t_i)}{N}\middle| N\right)\right] = E\left[\frac{N^2}{\overline{N}^2}p(1-p)\frac{1}{f_I N}\right] = p(1-p)\frac{1}{f_I \overline{N}}. \qquad \textbf{[S36]}$$

That is, the first term in Eq. **S33** is the error of a discrete sampling protocol with exactly $\overline{N}$ samples, as stated in the main text. The only effect of the expectation in the first term is to swap $\overline{N}$ for N. Dividing by the squared gain (Eq. **S30**), $d\bar{p}/d\mu_L = p(1-p)$, gives the first term in Eq. **2** in the main text and Eq. **S18** above.

We now turn to the second term in Eq. **S33**. From the law of total variance, this term describes how stochasticity in the number of samples, N, contributes to the sensing error. Because the number of samples N is Poisson with mean and variance equal to $\overline{N}$:

$$\mathrm{var}\left[\frac{N}{\overline{N}}E\left(\frac{\sum_{i=1}^{N} n(t_i)}{N}\middle| N\right)\right] = \mathrm{var}\left[\frac{N}{\overline{N}}p\right], \qquad \textbf{[S37]}$$

$$= \frac{p^2}{\overline{N}^2}\mathrm{var}[N], \qquad \textbf{[S38]}$$

$$= \frac{p^2}{\overline{N}}, \qquad \textbf{[S39]}$$

where the probability a receptor is bound is $E[n(t_i)] = p$. Dividing by the squared gain gives the second term in Eq. **2** in the main text and Eq. **S9** above. Thus, we have derived Eq. **2** in the main text as the result of a discrete sampling protocol.

The second term in Eq. **2** in the main text (i.e., Eq. **S9**) emerges in the derivations above as a consequence of the stochasticity in the number of samples N. However, it is more fundamentally a consequence of the fact that the cell does not distinguish between samples of the unbound receptor from blank samples that do not represent a receptor state—i.e., it does not distinguish x molecules that collided with the unbound receptor from those that never collided with the receptor in any state. A more standard sampling procedure would distinguish between these, and so would estimate $\hat{p}$ as $\hat{p} = x^*/N$, not $\hat{p} = x^*/\overline{N}$, as above. As we show in *Appendix C*, this procedure gives rise to only the first term of Eq. **2** in the main text, allowing us to interpret the second term as the price the cell pays for not distinguishing readout molecules that collide with the unbound receptor from those that have never collided with the receptor in any state.

The derivations leading to Eq. **S33** show that the sampling error for the sampling protocol must be the same as the sensing error for the biochemical network. To check this, we can calculate the sensing error for the biochemical network, Eq. **2** in the main text, in a more standard way, determining the gain and the variance of the output x^* and using Eq. **1** in the main text. This indeed gives exactly the same result.

Appendix B: Error of Discrete Sampling Protocols with a Fixed Number of Samples

In this section, we derive the first term of Eqs. **S31** and **S33**, corresponding to the first term of Eq. **2** in the main text (Eq. **S18**), as the error of a discrete sampling protocol with a fixed number of samples N taken of receptor states over time. The average receptor occupancy is estimated as the following:

$$\hat{p} = \frac{1}{N}\sum n_i(t_i), \qquad \text{[S40]}$$

where $n_i(t_i)$ is the state of the receptor involved in the ith sample at the time of that sample, 1, if the receptor was bound at time t_i, and 0, otherwise. In what follows, we consider a single receptor, $R_T = 1$ and $n(t_i) = n_i(t_i)$. The results generalize to multiple receptors. The times t_i of the samples represent the times at which the molecules that store the samples of the receptor collided with the receptor. Therefore, we choose the distribution of times between the samples to match the distribution of times between those collisions, which depends on the particular network under consideration, described below. We count time backward from the present time, $t = 0$. The number of samples N and the distribution of times at which they were taken specify a sampling protocol, independent of the chemical implementation.

The variance in the estimate of receptor occupancy is as follows:

$$\sigma_{\hat{p}}^2 = \mathrm{var}\left(\frac{\sum_{i=1}^{N} n(t_i)}{N}\right), \qquad \text{[S41]}$$

$$= \frac{\mathrm{var}\left(\sum_{i=1}^{N} n(t_i)\right)}{N^2}, \qquad \text{[S42]}$$

$$= \frac{\sigma^2}{N} + \frac{N(N-1)}{N^2} E\left[\mathrm{cov}\left(n(t_i), n(t_j)\right)\right], \qquad \text{[S43]}$$

because N is fixed, where $\sigma^2 = p(1-p)$ is the variance of the instantaneous occupancy of a single receptor.

Base Model with Activation Only, $x + RL \xrightarrow{k_f} x^* + RL$. We first consider a statistical sampling protocol that matches the distribution of receptor-collision times of samples in the base model. The collisions occur at random times in the interval $[0,T]$, so we model N randomly placed samples. The time $\tilde{\Delta}$ between a randomly chosen pair of uniformly distributed samples, not necessarily consecutive, is distributed as follows:

$$p(\tilde{\Delta}) = \frac{2}{T} - \frac{2\tilde{\Delta}}{T^2}. \qquad \text{[S44]}$$

Changing variables from t_i and t_j to $\tilde{\Delta} = |t_j - t_i|$, we have $\mathrm{cov}(n(t_i), n(t_j)) = \sigma^2 e^{-\tilde{\Delta}/\tau_c}$. The expectation of the covariance is then the following:

$$E\left[\mathrm{cov}\left(n(t_i), n(t_j)\right)\right] = \sigma^2 \int e^{-\tilde{\Delta}/\tau_c} p(\tilde{\Delta})\, d\tilde{\Delta}. \qquad \text{[S45]}$$

Assembling the equations above yields the first term in Eq. **2** in the main text (Eq. **S18**) with $\Delta = T/N$ ($R_T = 1$), where we have simplified the result with the standard assumption that $T \gg \tau_c$ and $N \gg 1$ (it does not make sense to discuss the spacing between a single sample).

Base Model with Activation Plus Deactivation, $x + RL \xrightarrow{k_f} x^* + RL$ and $x^* \xrightarrow{k_r} x$. To take into account deactivation, we consider sampling times which match the distribution of the receptor collisions of only those N molecules storing samples. We thus have to take into account that some of the samples that have been taken are thrown away due to the deactivation process. We begin with an alternative expression for the expected covariance:

$$E\left[\mathrm{cov}\left(n(t_i), n(t_j)\right)\right] = \sigma^2 \iint e^{-|t_j - t_i|/\tau_c} p(t_i, t_j) dt_i dt_j. \qquad \text{[S46]}$$

To match the biochemical network, the sample times t_i, t_j of two samples must be independent from each other, because the collisions of different molecules with the receptor and phosphatase are uncoupled. Therefore, $p(t_i, t_j) = p(t_i)p(t_j)$. The marginal probability $p(t_i)$ is the probability that the collision time with the receptor of a given molecule storing a sample was t_i, i.e., $p(t_i|\mathrm{sample})$. This can be written in terms of $p(\mathrm{sample}|t_i)$, the probability that there was a collision with the receptor at the time t_i times the probability that, given a collision at that time, the associated molecule did not subsequently collide with the phosphatase:

$$p(\mathrm{sample}|t_i)dt = r dt e^{-t_i/\tau_\ell}. \qquad \text{[S47]}$$

Then:

$$p(t_i|\mathrm{sample}) = \frac{p(\mathrm{sample}|t_i)\, p(t_i)}{\int p(\mathrm{sample}|t_i)\, p(t_i) dt_i} = \frac{1}{\tau_\ell} e^{-t_i/\tau_\ell}, \qquad \text{[S48]}$$

because $p(t_i)$ is uniform.

Assembling results:

$$E\left[\mathrm{cov}\left(n(t_i), n(t_j)\right)\right] = \sigma^2 \iint e^{-|t_j - t_i|/\tau_c} \frac{e^{-t_i/\tau_\ell}}{\tau_\ell} \frac{e^{-t_j/\tau_\ell}}{\tau_\ell} dt_i dt_j. \qquad \text{[S49]}$$

It is instructive to change variables, defining $\tilde{\Delta} = |t_j - t_i|$, as before. Then:

$$E\left[\mathrm{cov}\left(n(t_j), n(t_i)\right)\right] = \sigma^2 \int_0^\infty e^{-\tilde{\Delta}/\tau_c} \frac{e^{-\tilde{\Delta}/\tau_\ell}}{\tau_\ell} d\tilde{\Delta}. \qquad \text{[S50]}$$

From this expression we can identify $p(\tilde{\Delta}) = e^{-\tilde{\Delta}/\tau_\ell}/\tau_\ell$ as the distribution of times between two randomly chosen (not necessarily consecutive) samples, when molecules can decay. Simulations confirm this distribution.

Completing the integral and using it in the expression for the sensing error gives the first term in Eq. **2** in the main text (Eq. **S18**) for the effective spacing $\Delta = 2\tau_\ell/N$ (here, $R_T = 1$). We have made the simplifying assumptions that $N \gg 1$ (it does not make sense to talk of the spacing between just one sample) and $\tau_\ell \gg \tau_c$, a standard assumption. The effective spacing is not the mean nearest-neighbor spacing, but it is qualitatively similar and serves to summarize the fact that samples taken further apart in time are more independent. Clearly, from Eq. **S50**, the error depends on the distribution of all-pairs spacings, not necessarily nearest-neighbor spacings, and it depends on the full distribution, not just the mean.

Finally, we iterate that we can perform an independent check on the derivation in this section by computing the sensing error using the linear-noise approximation, which is exact for this linear network. As mentioned, this gives exactly the same result.

Appendix C: The Origin of the Second Term in Eq. 2 in the Main Text

The origin of the second term in Eq. **2** of the main text (i.e., Eq. **S18**) is that the cell cannot distinguish between those readout molecules that have collided with ligand-unbound receptors and readout molecules that have not collided with the receptors at all. One way to arrive at this conclusion is to imagine that all collisions with the receptor lead to modifications of x. However, although the ligand-bound receptor modifies x into state x^*, the unbound receptor modifies x into another state $x^\dagger$. Hence, in addition to the reaction $x + RL \to x^* + RL$, we consider the reaction

$x + R \to x^\dagger + R$. Then, $N = x^* + x^\dagger$. Analogously to Eq. **1** in the main text, we can then estimate the variance of $\hat{p} = x^*/N = x^*/(x^* + x^\dagger)$ by expanding to first order:

$$\delta\hat{p} \approx g_{\hat{p},x^*}\,\delta x^* + g_{\hat{p},x^\dagger}\,\delta x^\dagger, \qquad \textbf{[S51]}$$

where the gains are the following:

$$g_{\hat{p},x^*} = \frac{d\hat{p}}{dx^*} = \frac{x^*}{\left(x^* + x^\dagger\right)^2}, \qquad \textbf{[S52]}$$

$$g_{\hat{p},x^\dagger} = \frac{d\hat{p}}{dx^\dagger} = -\frac{x^\dagger}{\left(x^* + x^\dagger\right)^2}. \qquad \textbf{[S53]}$$

The variance is then the following:

$$\sigma^2_{\hat{p}} = g^2_{\hat{p},x^*}\,\sigma^2_{x^*} + g^2_{\hat{p},x^\dagger}\sigma^2_{x^\dagger} + 2g_{\hat{p},x^*}g_{\hat{p},x^\dagger}\sigma^2_{x^*,x^\dagger}, \qquad \textbf{[S54]}$$

where the last term accounts for the covariance. The variances can be calculated in many ways because the system is linear. For example, they can be calculated exactly via the linear-noise approximation. The result is the first term of Eq. **2** in the main text (Eq. **S18**), as claimed. Indeed, there is no second term for the model described here. This is precisely because with this scheme the number of samples N is known. Although in the scheme of the main text (Fig. 2), the system cannot discriminate between the molecules that have collided with an unbound receptor and the molecules that have not collided with the receptor at all, in this scheme the system knows exactly how many collisions there have been with the receptor: $x^* + x^\dagger$.

1. Milo R, Jorgensen P, Moran U, Weber G, Springer M (2010) BioNumbers—the database of key numbers in molecular and cell biology. *Nucleic Acids Res* 38(Database issue): D750–D753.
2. Sourjik V, Berg HC (2002) Binding of the *Escherichia coli* response regulator CheY to its target measured in vivo by fluorescence resonance energy transfer. *Proc Natl Acad Sci USA* 99(20):12669–12674.
3. Gardiner CW (1985) *Handbook of Stochastic Methods* (Springer, Berlin).
4. Ziv E, Nemenman I, Wiggins CH (2007) Effect of feedback on the fidelity of information transmission of time-varying signals. *PLoS One* 2(10):1077.
5. Berg HC, Purcell EM (1977) Physics of chemoreception. *Biophys J* 20(2):193–219.
6. Bialek W, Setayeshgar S (2005) Physical limits to biochemical signaling. *Proc Natl Acad Sci USA* 102(29):10040–10045.
7. Kaizu K, et al. (2014) The Berg-Purcell limit revisited. *Biophys J* 106(4):976–985.
8. Hill T (1977) *Free Energy Transduction in Biology: The Steady-State Kinetic and Thermodynamic Formalism* (Academic Press, New York).
9. Govern CC, ten Wolde PR (2012) Fundamental limits on sensing chemical concentrations with linear biochemical networks. *Phys Rev Lett* 109(21):218103.

Table S1. Molecular weights in amino acids are from ref. 1

Protein	Molecular weight, aa	Copy number
Tsr/Tar/Trg	~550	3,600–15,000
CheW	167	2,000–6,700
CheY	129	1,400–8,200
CheZ	214	560–3,200
CheA	654	1,100–6,700

Copy numbers are from ref. 2.

1. UniProt Consortium (2014) Activities at the universal protein resource (UniProt). *Nucleic Acids Res* 42(Database issue):D191–D198.
2. Li M, Hazelbauer GL (2004) Cellular stoichiometry of the components of the chemotaxis signaling complex. *J Bacteriol* 186(12):3687–3694.